# Self-Organization of Large Alumina Platelets and Silica Nanoparticles by Heteroaggregation and Sedimentation: Toward an Alternative Shaping of Nacre-Like Ceramic Composites

Manuella Cerbelaud, Mariana Muñoz, Fabrice Rossignol, Arnaud Videcoq

▶ **To cite this version:**

Manuella Cerbelaud, Mariana Muñoz, Fabrice Rossignol, Arnaud Videcoq. Self-Organization of Large Alumina Platelets and Silica Nanoparticles by Heteroaggregation and Sedimentation: Toward an Alternative Shaping of Nacre-Like Ceramic Composites. Langmuir, 2020, 36 (13), pp.3315-3322. 10.1021/acs.langmuir.0c00170 . hal-03035615

**HAL Id: hal-03035615**
**https://hal.science/hal-03035615**

Submitted on 3 Dec 2020

**HAL** is a multi-disciplinary open access archive for the deposit and dissemination of scientific research documents, whether they are published or not. The documents may come from teaching and research institutions in France or abroad, or from public or private research centers.

L'archive ouverte pluridisciplinaire **HAL**, est destinée au dépôt et à la diffusion de documents scientifiques de niveau recherche, publiés ou non, émanant des établissements d'enseignement et de recherche français ou étrangers, des laboratoires publics ou privés.

# Self-organization of large alumina platelets and silica nanoparticles by heteroaggregation and sedimentation: towards an alternative shaping of nacre-like ceramic composites

Manuella Cerbelaud,* Mariana Muñoz, Fabrice Rossignol, and Arnaud Videcoq

*Univ. Limoges, CNRS, IRCER, UMR 7315, F-87000 Limoges, France*

E-mail: manuella.cerbelaud@unilim.fr

**Abstract**

Nacre-like ceramic composites are of importance in a wide range of applications, because of their mechanical properties, combining high mechanical strength and high fracture toughness. Those mechanical properties are the result of strongly aligned platelets glued in a matrix. Different methods exist to shape such 'brick-and-mortar' hierarchical structure. In this paper, it is proposed to use the phenomenon of heteroaggregation between silica nanoparticles and large alumina platelets. Experimental and numerical results show that silica nanoparticles can adsorb on alumina platelets with a good distribution. This adsorption promotes the deagglomeration of alumina which can self-organize in layers by sedimentation. This phenomenon can be exploited to shape alumina-silica nacre-like composites.

# Introduction

During the last years, a special attention has been paid to nacre because of its mechanical properties combining both a high fracture strength and a high fracture toughness. This unusual combination of properties comes from the brick and mortar structure of nacre. Nacre is indeed comprised of 95vol% of well-aligned aragonite platelets (a crystallographic form of $CaCO_3$) glued together by 5vol% of organic materials (proteins and polysaccharides).[1] Different strategies are found in the literature to produce ceramic materials with such a hierarchical structure: use of magnetic particles alignment,[2] gluing of ceramic layers,[3] sedimentation[4] or more recently a series of filtration/compaction/sintering.[5] Bouville *et al.* have also used a method based on ice templating,[6] allowing a multi-scale self-organization in the final composite. After sintering, this final ceramic is composed of well-aligned alumina platelets glued in a glass matrix. To reinforce mechanical properties alumina nanoparticles are also introduced to create alumina bridges in between alumina platelets. For their shaping process, a suspension is then prepared with alumina platelets, alumina nanoparticles and with a silica-calcia suspension used as the glass precursor (nanoparticles of $\sim 20\,\mathrm{nm}$). To ensure the stability of this suspension, polymeric additives are added.[7] The presence of the polymers imposes then a phase of debinding during the sintering. And more generally, the presence of carbon residues in this system can be detrimental to final properties of consolidated parts.

To achieve the desired brick and mortar structure in the alumina-silica nacre-like ceramics, alumina platelets need to be aligned but also small silica particles must be well distributed in between to form an homogeneous intergranular phase (e.g. a vitreous phase) after sintering. In this paper, we propose to formulate suspensions composed of only alumina platelets and silica nanoparticles without any carbonated components, by using heteroaggregation. For that, we present a detailed study of the suspension behavior as a function of the mass ratio between the silica nanoparticles and the alumina platelets. To better understand the interactions between the components, both experimental characterizations and numerical

simulations are used. The objective of this study is to understand how such simple suspensions can be used as a base for shaping nacre-like ceramics.

# Methodology

## Experimental characterization

The alumina powder is a sapphire alumina named RonaFlair®White Sapphire from Merck, Germany (platelets with $d_{50}$ $\sim 7\mu$m, thickness$\sim$500 nm, purity $\geq$ 99%). Silica particles are taken from a commercial, aqueous suspension of Ludox TM50 provided by Grace Davison, United States (50 wt% $SiO_2$, $d_{50}$= 25 nm, purity 99.56%). An alkaline medium is used to stabilize this suspension with $Na^+$ as counterions. The mother suspension is diluted in osmosed water by 3 before use. Its pH is around 9. The mixed suspensions containing both alumina and silica are prepared in osmosed water. First alumina powder is introduced and then the dilute silica suspension is added. The whole suspension is then deagglomerated by an ultrasonic treatment (300 W, 30 s (pulse on 3 s, pulse off 1 s)).

Zeta potential measurements are carried out with an Acoustosizer IIs from Colloidal Dynamics. Suspensions are prepared in osmosed water with a solid loading of 1wt%. pH is adjusted manually with HCl 0.1 M and NaOH 0.1 M. The Smoluchowski model is used to estimate the zeta potential.

Sedimentation tests are carried out to evaluate the kinds of arrangements alumina platelets form. For that, 3 mL of alumina suspension prepared at 3vol% are allowed to settle in closed tubes during 24 hours. At the end, clear supernatants are obtained and the height of sediments is measured.

Microscopy observations are performed with a scanning electron microscope (SEM Quanta FEG 450 allowing the environmental mode). To observe sediments, a droplet of suspension taken in the middle of the sediment is deposited on a sample stub and is thus directly observed without any metallization in the environmental mode.

## Simulation methodology

In this paper, Brownian Dynamics simulations are performed to understand the interactions between the silica nanoparticles and the alumina platelets. In these simulations, the fluid is considered as a continuum medium and its effect on the particles is taken into account by introducing a friction term and a random term in the equation of Langevin, which is the equation of motion for a particle in suspension. By integrating this Langevin equation, the evolution of the particle positions can be described by:[8–10]

$$r_i(t+\delta t) = r_i(t) + \sqrt{(2D_i\delta t)}\ \ Y_i + \frac{D_i}{k_{\mathrm{B}}T}\sum_j F_{ij}\{r_{ij}(t)\}\delta t \tag{1}$$

with $r_i$ the mass center of particle $i$, $D_i$ the diffusion coefficient of particle $i$, $\delta t$ the time step of simulation, $r_{ij}$ the center-to-center distance between particles $i$ and $j$, $k_{\mathrm{B}}$ the Boltzmann's constant and $T$ the temperature. $Y_i$ is an uncorrelated Gaussian distributed random number with an average of 0 and a variance equal to 1. $F_{ij}\{r_{ij}(t)\}$ are the pair interaction forces applied on particle $i$ that will be derived from the pair interaction potentials ($F_{ij} = -\nabla V_{ij}$). Because of the huge size ratio between the silica and the alumina particles ($\sim$ 300 to 400), taking into account both kinds of particles in a simulation is too cumbersome. Therefore two kinds of simulations are used: the first one is used to study the behavior of silica particles close to an alumina platelet and the second one to study the behavior of several alumina platelets without considering explicitly the silica particles.

**Silica particles in the vicinity of alumina** To model the alumina surface, which is in fact plane, it was chosen to use a wall of the simulation box, and interactions between the silica nanoparticles and alumina are considered as sphere-plane interactions. Brownian dynamics simulations are then performed with 1000 silica nanoparticles of 25 nm diameter

using an Ermak algorithm[8] (see Eq 1). The diffusion coefficient for a sphere is given by:

$$D_{sphere} = \frac{k_{\mathrm{B}}T}{6\pi\eta a} \tag{2}$$

with $\eta$ the solvent viscosity (here for water $\eta = 10^{-3}\,\mathrm{Pa.s}$) and $a = 12.5\,\mu\mathrm{m}$ the radius of silica particles. Simulations are carried out at $T = 293\,\mathrm{K}$ with a time step of $\delta t = 5.10^{-10}\,\mathrm{s}$. A cubic simulation box is used with periodic conditions in 'x' and 'y' directions. The upper wall in 'z' direction is a repulsive wall, modelled by a linear repulsive interaction. The lower wall in 'z' direction represents the alumina surface. Interactions in this system are modelled by a DLVO potential[11,12] (Derjaguin, Landau, Verwey and Overbeek), which has already been successfully used to describe interactions between alumina and silica particles.[13,14] This potential is the sum of two different contributions: one due to the attractive van der Waals interaction and the other due to the electrostatic interaction. To model the silica nanoparticle interactions, the expression developed for spheres is used. The van der Waals contribution is then expressed as:[15]

$$V_{ij}^{sphere-sphere-vdW} = -\frac{A_{ss}}{6}\left[\frac{2a^2}{r_{ij}^2 - 4a^2} + \frac{2a^2}{r_{ij}^2} + \ln\left(\frac{r_{ij}^2 - 4a^2}{r_{ij}^2}\right)\right] \tag{3}$$

where $A_{ss}$ is the Hamaker constant (for silica in water $A_{ss} = 4.6 \times 10^{-21}\,\mathrm{J}$[16]), $a$ the particle radius (here $a = 12.5\,\mathrm{nm}$) and $r_{ij}$ the center-to-center distance between particles $i$ and $j$. For the interaction between silica particles and the bottom wall in 'z' direction, representing the alumina surface, the interaction developed for a sphere and an infinite plane is used:[15]

$$V_{i}^{sphere-plane-vdW} = -\frac{A_{as}}{6}\left[\frac{a}{h_i} + \frac{a}{h_i + 2a} + \ln\left(\frac{h_i}{h_i + 2a}\right)\right] \tag{4}$$

where $A_{as}$ is the Hamaker constant for alumina-silica interactions in water (here $A_{as} = \sqrt{A_{ss}A_{aa}} = \sqrt{4.6 \times 10^{-21} \times 4.76 \times 10^{-20}} = 1.48 \times 10^{-20}\,\mathrm{J}$[16]) and $h_i$ the surface-to-surface distance between the particle $i$ and the plane.

For the electrostatic interactions between the silica particles, the Hogg-Healy-Fuerstenau (HHF) potential developed for spheres is used:

$$V_{ij}^{sphere-sphere-HHF} = \pi\epsilon a\psi^2 \left[\ln\left(\frac{1+\exp(-\kappa h_{ij})}{1-\exp(-\kappa h_{ij})}\right) + \ln\left(1-\exp(-2\kappa h_{ij})\right)\right] \tag{5}$$

where $\kappa$ is the inverse Debye length (here no salt is added and $\kappa = 10^8\,\mathrm{m}^{-1}$), $\psi$ is the surface potential of the particles (assimilated here to the zeta potential), $h_{ij}$ the surface-to-surface distance between particles $i$ and $j$. For the interaction between the alumina and the silica, the general HHF expression for two spheres is used by modifying it in such a way that one of the radii approaches infinity:[15]

$$V_{ij}^{sphere-plane-HHF} = \pi\epsilon a\left(\psi_i^2+\psi_j^2\right)\left[\frac{2\psi_i\psi_j}{\psi_i^2+\psi_j^2}\ln\left(\frac{1+\exp(-\kappa h_{ij})}{1-\exp(-\kappa h_{ij})}\right) + \ln\left(1-\exp(-2\kappa h_{ij})\right)\right] \tag{6}$$

Because DLVO potential becomes infinite at the contact, it is cut at $-14k_{\mathrm{B}}T$ to avoid divergence and a linear repulsive potential is added to avoid interpenetration. This value of cut-off has been chosen because it has already allowed to reproduce the adsorption of silica nanoparticles on $\alpha$-alumina quasi spherical particles.[13,17] At the beginning of the simulation, silica particles are randomly placed in a cubic simulation box by avoiding overlapping with the other ones and with the walls in z-direction.

**Behavior of alumina platelets** Brownian dynamics simulations are also used to study the packing of alumina platelets during sedimentation. To take into account their specific morphology, alumina platelets are modelled as a non-deformable assembly of 153 spheres of diameter $d_{el} = 500\,\mathrm{nm}$ (see Figure 1), which corresponds to the thickness of the sapphire platelets. Brownian dynamics is performed as in References 10 and 18, taking into account

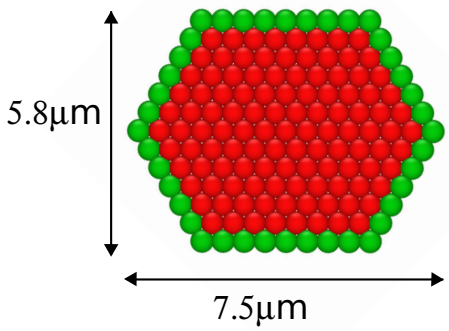


Figure 1: Modelling of an alumina platelet by an assembly of 153 elementary spheres of 500 nm. For visibility the edges are represented by an other color.

both translation (equation 1) and rotation motions by following the angle variation:

$$\Delta\theta_i = (2D_r\delta t)^{1/2}Y_i + \frac{D_r T_i}{k_{\mathrm{B}}T}\delta t \tag{7}$$

$T_i$ is the torque induced by the interactions on particle $i$ and $D_r$ is the rotational diffusion coefficient of particle $i$. Alumina platelets are assimilated to a disk of radius $a_d = 3.325\,\mu$m (disk of equivalent surface). Thus the translational diffusion coefficient to is expressed as:[19]

$$D_{translation} = \frac{k_{\mathrm{B}}T}{12\eta a_d} \tag{8}$$

and the rotational diffusion coefficient as:

$$D_{rotation} = \frac{3k_{\mathrm{B}}T}{32\eta a_d^3}. \tag{9}$$

In these simulations, silica nanoparticles are not explicitly represented. However, the presence of them obviously modify the interaction between the platelets. To understand this effect, an effective Yukawa potential is used for the interactions between the elementary spheres constituting the platelets, allowing to tune the degree of interaction by modifying

both the sign ($sign$ is + for repulsion or - for attraction) and the well-depth value $U^*$:

$$V^{Yukawa} = (sign)U^* \frac{d_{el}}{r_{kl}} \exp\left(-\kappa(r_{kl} - d_{el})\right) \tag{10}$$

where $r_{kl}$ is the center-to-center distance between the elementary spheres $k$ and $l$. At contact, this potential is cut and linear repulsive interactions are introduced between elementary spheres to avoid interpenetration. Interactions on an alumina particle are then obtained by summing all the interactions applied on its beads and the torque induced by the bead-bead interaction is obtained by:

$$T_i = \sum_{k \in i} d_k \sum_{l \notin i} F_{kl}\{r_{kl}(t)\} \tag{11}$$

with $d_k$ the distance vector between the bead $k$ belonging to the platelet $i$ and the center of the alumina platelet $i$.

To model sedimentation, gravity is applied to the platelet center as a force (central force):

$$F = (\rho_{al} - \rho_{water}) V_{platelet} g \tag{12}$$

with $\rho_{al}$ the density of alumina ($3980\,\mathrm{kg.m^{-3}}$), $\rho_{water}$ the density of water ($1000\,\mathrm{kg.m^{-3}}$), $V_{platelet}$ the platelet volume ($1.73 \times 10^{-17}\,\mathrm{m^3}$), and $g$ the standard gravity.

A parallelepiped with square base, whose 'z' dimension is 5 times larger than 'x' or 'y' dimensions, is used as simulation box. Periodic boundary conditions are considered in 'x' and 'y' directions and walls in 'z' direction, using a repulsive interaction:

$$V^{rep} = k_{\mathrm{B}} T \left(\frac{2a_d}{h + a_d}\right)^{12} \tag{13}$$

Simulations are performed with 150 platelets. Because of the large amount of elementary spheres, simulations are parallelized thanks to a home-made code developed for calculations on GPU (Graphics Processing Unit).[20] A time step of $10^{-7}\,\mathrm{s}$ is used and analyses are done at $t = 20\,\mathrm{s}$.

# Results and discussion

## Behavior of the alumina suspensions

To understand the behavior of alumina suspensions, experimental characterizations are carried out. The evolution of the zeta potential as a function of pH is reported in Figure 2 for the alumina platelets. Alumina platelets have an isoelectric point (IEP) around 9, simi-

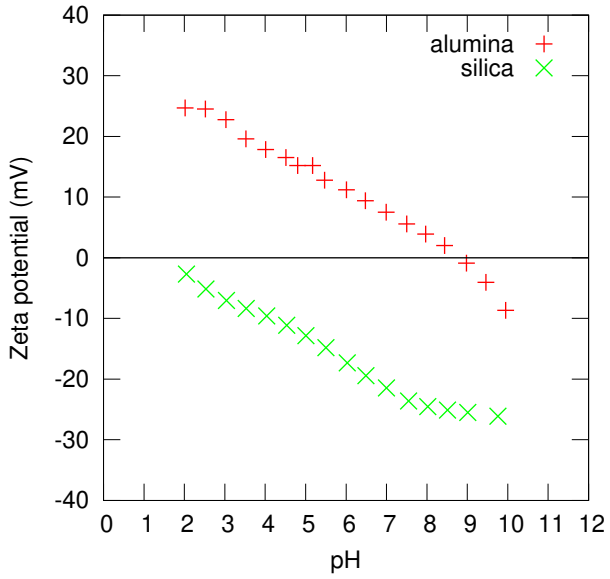


Figure 2: Zeta potentials of alumina and silica as a function of pH.

larly to $\alpha$-alumina particles.[13] In the literature, it is reported that sapphire has normally a lower IEP around 6, which is generally explained by the different types of hydroxyl groups found on the surface, especially on the (0001) plane.[21] These groups dissociate at different pKa forming an amphoteric particle with negatively charged basal planes. This behavior is not observed for the commercial powder used in this study, which let us think that the surface of this powder is more similar to the $\alpha$-alumina one. It has indeed been reported that (0001) sapphire plane can have an IEP similar to $\alpha$-alumina after being treated with oxygen plasma.[21] That is why, in this study, below pH 9 edges and faces of platelets are considered as positively charged and above pH 9 as negatively charged. Figure 3 shows the

results of sedimentation tests performed at different pH for 3vol% alumina suspensions. The

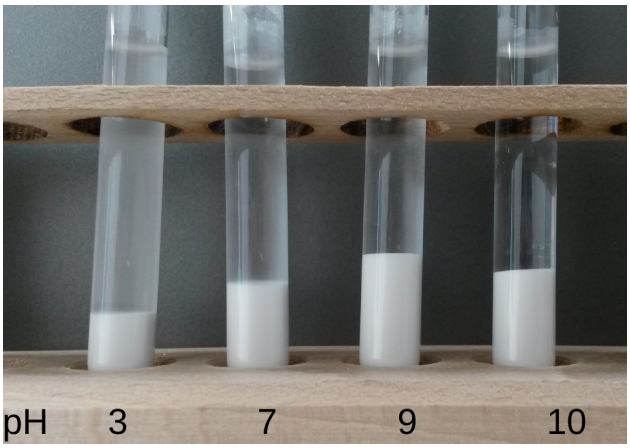


Figure 3: Picture at 24 h of the closed tubes used for the sedimentation tests of alumina suspensions prepared at different pH.

height of the sediment increases until pH 9 and then decreases at pH 10. This behavior is similar to the $\alpha$-alumina behavior and can be linked to the zeta potential measurements. From pH 3 to pH 9, the zeta potential of particles decreases, the suspension becomes more and more instable and the sediment height increases. At pH 10, the pH is higher than the IEP, particles are thus negatively charged and suspension begins to be again more stable. This behavior is in agreement with our hypothesis that edges and faces of alumina can be considered as similarly charged. It should be noted that, at pH<9, the tubes are not clear above the sediment. At these pH, particles tend to stick to the glass tube, which also reflects the positive charge of the particles.

## Silica adsorption onto alumina platelets

The evolution of the zeta potential as a function of pH for the silica nanoparticles is also reported in Figure 2. On the whole pH range, silica is found negatively charged, therefore heteroaggregation between alumina and silica is expected over a wide range of pH [2 - 8]. To understand the effect of silica addition on the alumina particles, acoustophoresis measurements are carried out on an alumina suspension in which silica nanoparticles are progressively added. Figure 4 shows the variation of both pH and zeta potential as a function

of the amount of added silica $R$ defined as $R = m_{SiO_2}/m_{Al_2O_3}$ with $m_{SiO_2}$ the mass of silica and $m_{Al_2O_3}$ the mass of alumina. The natural pH of alumina suspension is found around 6.

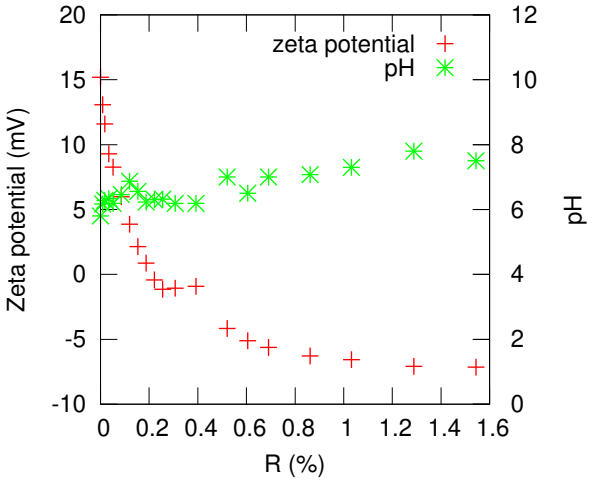


Figure 4: Evolution of the zeta potential and of the pH as a function of the silica content $R$ introduced in the alumina suspension.

It increases until 7.5 with the silica addition (Cf. silica suspension has a pH of 9), but in all cases for these pH, alumina and silica are oppositely charged and heteroaggregation is therefore expected. In parallel, the addition of silica leads to a decrease of the zeta potential of alumina. For a ratio $R \gtrsim 0.4\%$, the zeta potential becomes even negative. The change of zeta potential is explained by the adsorption of the silica nanoparticles on the alumina platelets, because of their opposite charges. This adsorption is indeed observed by electron microscopy as shown in Figure 5. In addition, the picture shows that the basal planes of alumina are covered by the silica nanoparticles, confirming that these latest are positively charged. Figure 4 shows also, that with $R \gtrsim 1.3\%$, the zeta potential does not vary anymore. This concentration seems to correspond to a saturation of adsorption. Considering that for this amount, all the nanoparticles are absorbed and that platelets can be modeled by 500 nm thick and 6.65$\mu$m of diameter cylinder, it is found that around 630 silica nanoparticles are adsorbed per $\mu$m$^2$.

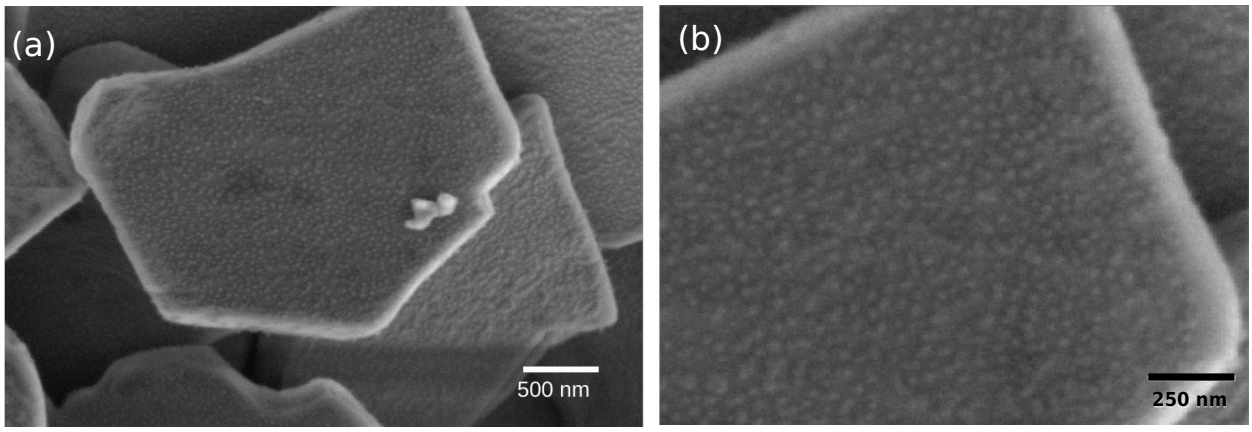


Figure 5: SEM picture taken in environmental mode of a sediment obtained with alumina platelets and silica nanoparticles ($R$=3%, pH$\sim$ 8). (b) is an inset of (a). Alumina platelets are homogeneously covered by silica nanoparticles.

In parallel, the adsorption of the nanoparticles on the alumina is studied by Brownian dynamics simulations. According to Figure 2, at pH 7 a surface potential of $-21$ mV is used for the silica and of 7 mV for the alumina. The DLVO potentials obtained with these values are shown in Figure 6. An attraction is obtained for the alumina-silica interaction, whereas silica particles repulse each other. The barrier of this potential is low (around $3.5k_{\mathrm{B}}T$) however repulsion is found over a long distance ($5.5a$). Figure 7 shows the results of simulations. During the simulation, the nanoparticles are attracted towards the bottom wall and after 0.0075 s there is no more evolution of the adsorption. Many nanoparticles remain in the bulk and a saturation of the adsorption is obtained. It is observed that adsorbed silica nanoparticles do not touch each other, which is in agreement with the SEM observations (Figure 5). This can be explained by the repulsion existing between these nanoparticles. The number of adsorbed nanoparticles has been evaluated as an average over 10 independent simulations. It is found that around 690 nanoparticles/$\mu$m$^2$ are adsorbed. This value is slightly higher than the experimental one, however it corresponds in both cases to a low coverage of the alumina surface. This difference can be explained on the one hand by different approximations done to evaluate the amount of adsorbed silica particles in experiments (shape and size of alumina platelets), and on the other hand by numerical approximations, such as the value

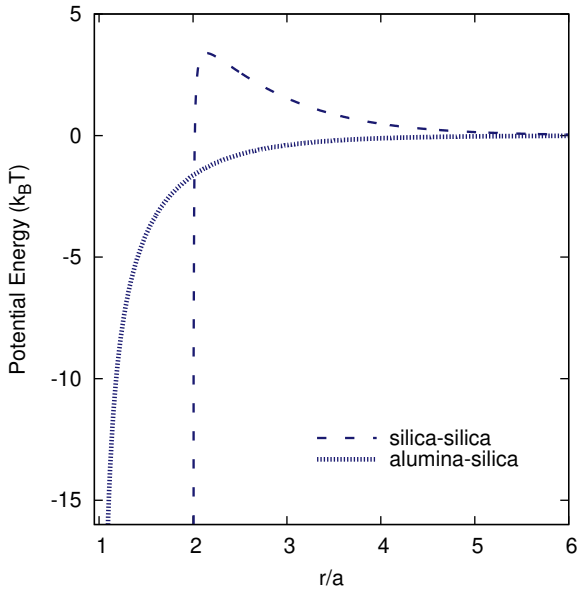


Figure 6: DLVO potentials used for silica-silica interactions (sphere-sphere) and silica-alumina interaction (sphere-plane) as a function of the dimensionless distance ($(r/a)$ with $r$ the center-to-center distance between spheres or the center-to-surface distance between a sphere and a plane, $a$ the radius of silica nanoparticles.)

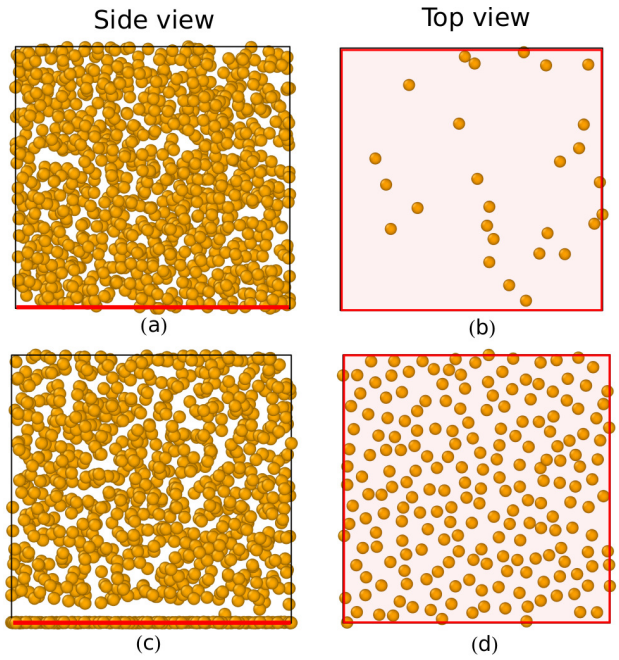


Figure 7: Snapshots of Brownian dynamics simulations used to analyze the adsorption of silica nanoparticles onto alumina. Initial conditions: (a) picture of the box and (b) sliced view of the bottom wall. Results of simulations at $t = 0.0075\,\mathrm{s}$: (c) picture of the box and (d) sliced view of the bottom wall.

of the cut-off or the infinite wall. However, these results confirm that, in order to explain adsorption, on the one hand basal planes of alumina particles must have positive charges for the silica nanoparticles to adsorb, and, on the other hand, repulsions between those silica particles lead to a rather low but very homogeneous coverage of alumina platelets. Moreover, using the zeta potential as surface potential seems to be a good approximation for the whole alumina particles.

## Sedimentation of silica covered alumina platelets

The effect of Ludox addition on the platelet arrangement is observed by sedimentation tests. Figure 8 shows the picture of the tubes obtained after sedimentation in presence of different amount of silica $R$. The values of the solid volume fraction in the sediments

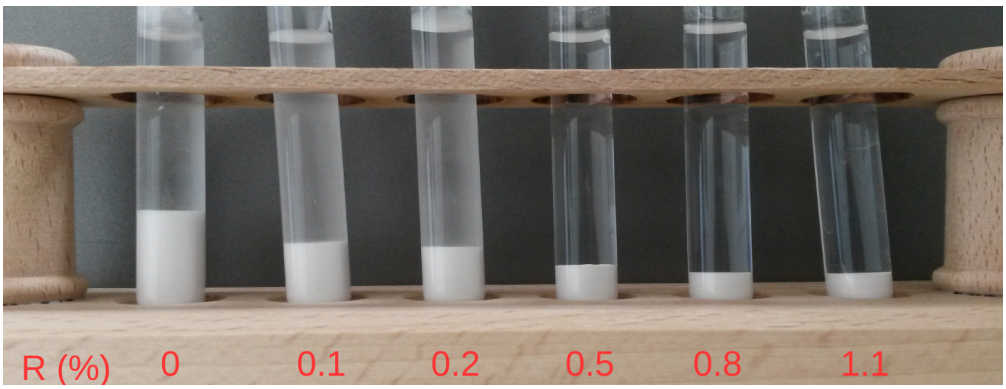


Figure 8: Picture of the closed tubes used for the sedimentation tests taken 24 h after preparation. $R$ represents the silica amount added in the tube.

($\phi_s = particle\,volume/sediment\,volume$), are reported in Table 1.

It is observed that increasing the silica content increases the volume fraction of particles in the sediment. When no silica is added, the solid volume fraction in the sediment is measured at $\phi_s = 8\%$, but when $R = 1.1\%$, this value is multiplied by 3.5 leading to a volume fraction of $\phi_s = 28\%$. This value is greater than those obtained for suspensions of alumina alone at any pH, for which the largest volume fraction in the sediment is obtained

Table 1: Values of the sediment height ($h_s$) and of the solid volume fraction in the sediments $\phi_s$ measured in the sedimentation tests. The left hand side corresponds to Figure 8 and the right hand side to Figure 3.

| Alumina-Silica | | | Alumina | | |
|---|---|---|---|---|---|
| R(%) | $h_s$ ±0.5 (mm) | $\phi_s$±2.5 (%) | pH | $h_s$ ±0.5 (mm) | $\phi_s$±2.5 (%) |
| 0 | 18 | 8 | 3 | 11 | 13 |
| 0.1 | 13 | 11 | 7 | 18 | 8 |
| 0.2 | 10 | 14 | 9 | 22 | 6 |
| 0.5 | 7 | 20 | 10 | 18 | 8 |
| 0.8 | 5 | 28 | | | |
| 1.1 | 5 | 28 | | | |

at pH 3 ($\phi_s = 13\%$), which corresponds to the highest value of alumina zeta potential. Moreover, sedimentation tests also show that, for $R < 0.5\%$, the tubes are not clear above the sediment. This is due to particles that stick to the glass tube and can be explained by the presence of positive charges on the alumina particles, in agreement with zeta potential measurements (see Figure 4). For $R \geq 0.5\%$, the tube walls are clear. According to the acoustophoresis measurements, for these ratios, alumina particles are sufficiently covered by silica to appear as negatively charged.

Let us now discuss the effect of the adsorbed silica on the alumina interactions. Because of its low surface potential (7 mV), electrostatic repulsions between alumina platelets are weak and they should aggregate because of the van der Waals attraction. When silica nanoparticles begin to adsorb on alumina, first they can counterbalance the van der Waals attraction between platelets because of steric effects and then, because of their negative charges, they can cause the alumina particles to progressively repel each other as a result of electrostatic repulsion. Because silica nanoparticles adsorb on alumina, depletion effects are unlikely. As the repulsion between silica-covered alumina platelets increases, it is observed that the sediment packing density increases, which means that the platelets alignement in the sediment increases as well.

Brownian dynamics simulations performed on platelets with interactions that vary from attractive to repulsive allow to well understand this phenomenon. At the beginning particles

are first dispersed in the simulation box and then they are allowed to settle under gravity during the simulation (see Figure 9). The volume fraction of particles is fixed at 2.2vol%, the maximum fraction avoiding preferential orientations during the generation of the initial random positions. It takes around 10 s to obtain a sediment composed of all particles at

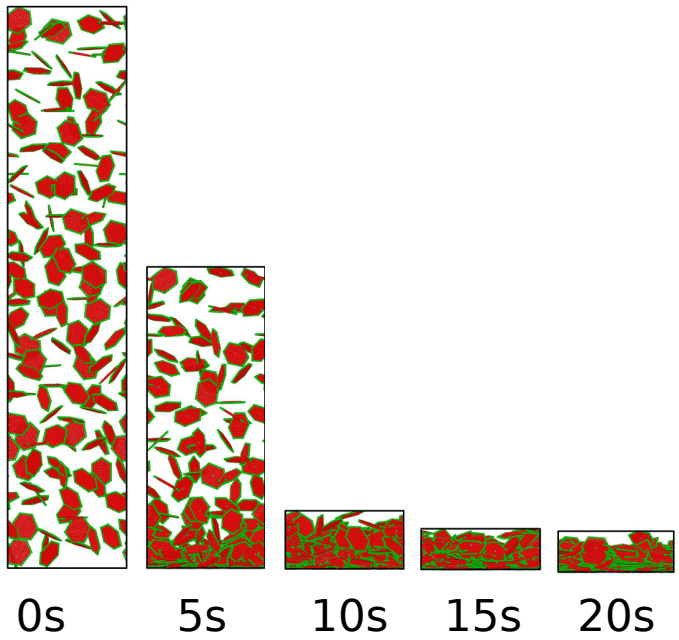


Figure 9: Snapshots of Brownian dynamics simulations used to analyze the sedimentation of alumina platelets.

the bottom of the box. Then, small reorganization occur in the sediment. At $t = 20\,\mathrm{s}$, the sediment height does not evolve significantly and analysis is then performed. Even if hydrodynamic interactions are not taken into account, numerical results allow to qualitatively understand the suspension behavior. Simulations are carried out with Yukawa potential for $(sign)U^*$= -160, -30 and $30k_\mathrm{B}T$ (Cf. Equation 10) to mimic a progressive addition of silica. Results are shown in Figure 10.

The sediment height decreases when alumina particles are less and less attractive, in agreement with the sedimentation tests. For strongly attractive particles, the volume fraction of solid in sediments is of 18%, but it arrives to around 40% for the case where particles are repulsive. This increase is due to the compactness of the particle set, which is linked to their orientation in the sediment. The evaluation of the platelet orientations, performed by

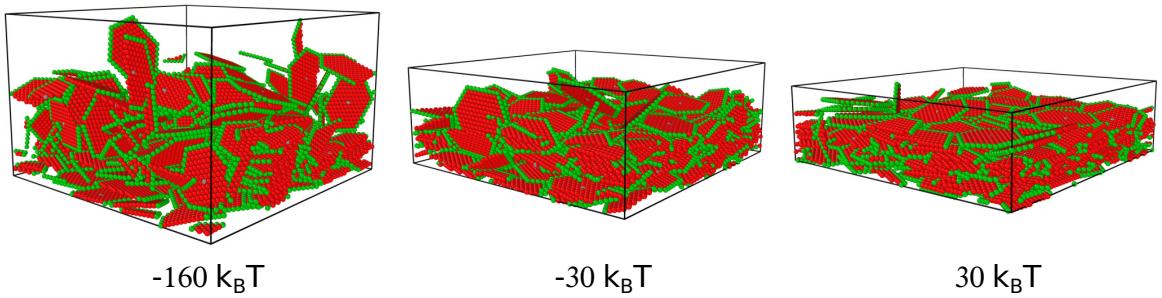


Figure 10: Snapshots of Brownian dynamics simulations at 20 s for $(sign)U^*$= -160, -30 and $30k_{\mathrm{B}}T$.

measuring the angles formed by the platelets and the bottom plane, is reported in Figure 11.

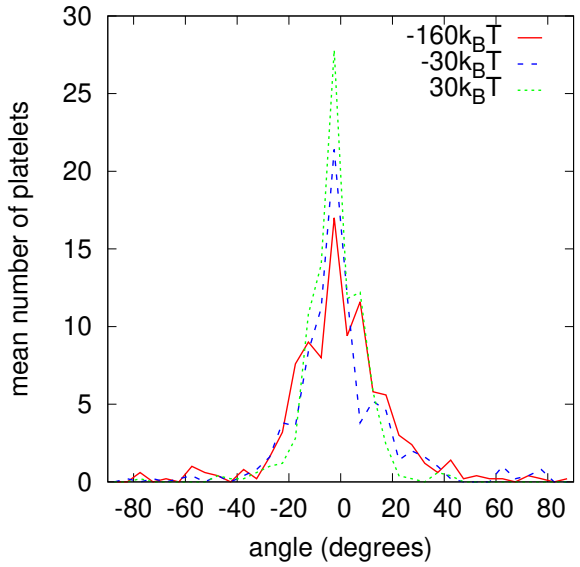


Figure 11: Angle distribution of platelets in sediments at $t = 20$ s for the different values of $(sign)U^*$ used in the Yukawa potential: -160, -30 and $30k_{\mathrm{B}}T$. Distribution is obtained from histograms constructed with an angle range of $5^o$. An angle of 0 means that the platelet is aligned with the bottom wall of the simulation box. Results are averaged over 5 independent simulations.

For strongly attractive particles, a wider angle distribution is observed. When particles encounter each other, they indeed strongly stick together, whatever their mutual orientation. In this case, an 'house-of-card' structure is obtained. When attraction is decreased, the re-organization between particles is easier, which gives a higher packing density. And when particles become repulsive, particles do not stick to each other and are thus better aligned

in the bottom plane by gravity.

The very good platelet alignment achieved both experimentally and in simulations let us think that this kind of system might be very interesting to form artificial nacre, and therefore that adding silica nanoparticles to alumina could be a good strategy. Moreover, as observed previously, since silica nanoparticles are attracted towards platelets and repel each other, a good distribution of silica on the alumina platelets can be achieved, which should lead to a good homogeneity of the final body composition.

# Conclusion

In this paper, a detailed study of the behavior of aqueous suspensions composed of RonaFlair®White Sapphire (alumina platelets) and Ludox TM50 (silica nanoparticles) is presented. Because of the surface properties of the alumina platelets, heteroaggregation with silica is possible for a pH around 7. At this pH, the negatively charged silica nanoparticles adsorb on the positively charged alumina platelets. The saturation of adsorption appears for a low concentration of silica ($R \sim 1.3\%$), which is due to the repulsion between the silica nanoparticles. The alumina platelets are not fully covered, however a good distribution of silica nanoparticles on them is obtained. Moreover, the presence of these adsorbed silica nanoparticles leads to the dispersion of the initially flocculated alumina suspension due to their size and their surface potentials. The sedimentation of such mixed suspensions, where silica nanoparticles are fixed onto the large platelets, is quite fast, and gives sediments where particles can be very well aligned. To conclude, this study opens perspectives to shape well structured alumina-silica nacre-like composites without using carbonated additives such as dispersing agents that would have to be removed through debinding afterwards, resulting in some potential detrimental residues.

# Acknowledgements

This work is supported by institutional grants from the French National Agency of Research (ANR-16-CE08-0006-0A BICUIT project). The authors want to acknowledge Sylvain Deville from the Ceramic Synthesis and Functionalization Laboratory (UMR 3080 CNRS-Saint-Gobain) for providing the alumina powder, and all of the members of the ANR BICUIT consortium for the fruitful discussions. The authors thank also CALI and its team for providing the computational facilities (CALI has been financed by the region Limousin, the institutes XLIM, IPAM, GEIST, and the University of Limoges). Figures 1, 7, 10 and 9 have been obtained thanks to the software OVITO.[22]


# References


(1) Sun, J.; Bhushan, B. Hierarchical structure and mechanical properties of nacre: a review. *RSC Advances* **2012**, *2*, 7617–7632, DOI: 10.1039/C2RA20218B.

(2) Le Ferrand, H.; Bouville, F.; Niebel, T.; Studart, A. Magnetically assisted slip casting of bioinspired heterogeneous composites. *Nat. Mater.* **2015**, *14*, 1172–1179, DOI:10.1038/nmat4419.

(3) Clegg, W.; Kendall, K.; McN Alford, N.; Button, T.; Birchall, J. A simple way to make tough ceramics. *Nature* **1990**, *347*, 455–457, DOI: 10.1038.

(4) Behr, S.; Vainio, U.; Müller, M.; Schreyer, A.; Schneider, G. A. Large-scale parallel alignment of platelet-shaped particles through gravitational sedimentation. *Sci. Rep.* **2015**, *5*, 9984, DOI: 10.1038/srep09984.

(5) Magrini, A.; Bouville, F.; Lauria, A.; Ferrand, H. L.; Niebel, T.; Studart, A. Transparent and tough bulk composites inspired by nacre. *Nature Communications* **2019**, *10*, 2794, DOI: 10.1038/s41467–019–10829–2.

(6) Bouville, F.; Maire, E.; Meille, S.; de Moortèle, B. V.; Stevenson, A.; Deville, S. Strong, tough and stiff bioinspired ceramics from brittle constituents. *Nat. Mater.* **2014**, *13*, 508–514, DOI: doi.org/10.1038/nmat3915.

(7) Bouville, F. Self-assembly of anisotropic particles driven by ice growth : Mechanisms, applications and bioinspiration. Ph.D. thesis, 2013; Thèse de doctorat dirigée par Deville, Sylvain et Maire, Eric: Matériaux Lyon, INSA 2013.

(8) Ermak, D.; McCammon, J. Brownian dynamics with hydrodynamic interactions. *J. Chem. Phys.* **1978**, *69*, 1352–1360, DOI: 10.1063/1.436761.

(9) Allen, M.; Tildesley, D. *Computer Simulation of Liquids*; Oxford Science Publications, 1987.

(10) Cerbelaud, M.; Lestriez, B.; Videcoq, A.; Ferrando, R.; Guyomard, D. Understanding the structure of electrodes in Li-ion batteries: a numerical study. *J. Electrochem. Soc.* **2015**, *162*, A1485–A1492, DOI: 10.1149/2.0431508jes.

(11) Derjaguin, B.; Landau, L. Theory of the stability of strongly charged lyophobic sols and of the adhesion of strongly charged particles in solution of electrolytes. *Acta Physicochim. URSS* **1941**, *14*, 633–662, DOI: 10.1016/0079–6816(93)90013–L.

(12) Verwey, E.; Overbeek, J. *Theory of the Stability of Lyophobic Colloids*; Elsevier: Amsterdam, 1948.

(13) Cerbelaud, M.; Videcoq, A.; Abélard, P.; Pagnoux, C.; Rossignol, F.; Ferrando, R. Heteroaggregation between $Al_2O_3$ submicrometer particles and $SiO_2$ nanoparticles : Experiments and simulation. *Langmuir* **2008**, *24*, 3001–3008, DOI: 10.1021/la702104u.

(14) Cerbelaud, M.; Videcoq, A.; Abélard, P.; Pagnoux, C.; Ferrando, R. Self-assembly of oppositely charged particles in dilute ceramic suspensions: predictive role of simulations. *Soft Matter* **2010**, *6*, 370–382, 10.1039/B908671D.

(15) M.Elimelech,; Gregory, J.; Jia, X.; Williams, R. *Particle deposition & Aggregation. Measurement, modelling and simulation*; Butterworth-Heinemann Ltd: Oxford, England, 1995.

(16) Bergström, L. Hamaker constants for inorganic materials. *Adv. Colloid Interface Sci.* **1997**, *70*, 125–169, DOI: 10.1016/S0001–8686(97)00003–1.

(17) Cerbelaud, M.; Videcoq, A.; Abélard, P.; Ferrando, R. Simulation of the heteroagglomeration between highly size-asymmetric ceramic particles. *J. Colloid Interface Sci.* **2009**, *332*, 360–365, DOI: 10.1016/j.jcis.2008.11.063.

(18) Cerbelaud, M.; Lebdioua, K.; Tran, C. T.; Crespin, B.; Aimable, A.; Videcoq, A. Brownian dynamics simulations of one-patch inverse patchy particles. *Phys. Chem. Chem. Phys.* **2019**, *21*, 23447–23458 DOI: 10.1039/C9CP04247D.

(19) Holmqvist, P.; Meester, V.; Westermeier, F.; Kleshchanok, D. Rotational diffusion in concentrated platelet systems measured with X-ray photon correlation spectroscopy. *J. Chem. Phys.* **2013**, *139*, 084905,DOI: 10.1063/1.4818532.

(20) Tran, C. T.; Crespin, B.; Cerbelaud, M.; Videcoq, A. Brownian Dynamics Simulation on the GPU: Virtual Colloidal Suspensions. Workshop on Virtual Reality Interaction and Physical Simulation. 2015; pp ,DOI: 10.2312/vriphys.20151332.

(21) Franks, G.; Gan, Y. Charging behavior at alumina-water interface and implications for cermic processing. *J. Am. Ceram. Soc.* **2007**, *90*, 3373–3388, DOI: 10.1111/j.1551–2916.2007.02013.x.

(22) Stukowski, A. Visualization and analysis of atomistic simulation data with OVITO-the Open Visualization Tool. *Modelling Simul. Mater. Sci. Eng.* **2010**, *18*, 015012, DOI:10.1088/0965–0393/18/1/015012.

# Table of Contents